

Supporting information

A Cost-Effective and Innovative Detector for Iron Ions

Yanhui Guo, Jiayi Zhu, Yumei Dai, Long Chen, Weibing Li, Zihang Yuan, Jie Zhou, En Tang*

Corresponding addresses: tangen@mku.edu.cn

Minnan Science and Technology University, Fujian, 362000, China

Due to the relatively large distance of the free water molecules from the primary structure, they were subtracted using a solvent mask for ease of mapping and to simplify the structure. Additionally, 1.1 water molecules were added to the molecular formula. This represents merely an estimate of the number of electrons computed from the solvent masking performed by the software. The molecular formula is $C_{30}H_{26.2}N_4O_{12.1}Zn_2$.

Table. S1 Crystallographic data and structure refinement

chemical formula	$C_{30}H_{24}N_4O_{11}Zn_2$	V/nm^3	2991.08(254)
relative molecular mass	747.27 g/mol	Z	4
Space group	P 1 21/c 1 (14)	$\rho /g.cm^{-3}$	1.659
crystal system	monoclinic crystal	absorption coefficient μ/mm^{-1}	1.674
a/ Å	22.1729(9)	F(000)	1520
b/ Å	8.4424(4)	R1, wR values ($I > 2\sigma(I)$)	0.0583,0.1836
c/ Å	17.3538(6)	R1, wR values (all data)	0.0840,0.2049
$\alpha/^\circ$	90	The goodness of fit of F2.	1.048
$\beta/^\circ$	112.96(0)	θ range	3.51-29.64
$\gamma/^\circ$	90	Peak and pore with the maximum difference ($e \cdot nm^{-3}$)	2.971 , -0.703

Table. S2 Bond lengths [Å] and angles [deg]

chemical bond	bond length /nm	chemical bond	bond length /nm
Zn1—O1	2.417(4)	Zn2—O6	2.000(3)
Zn1—N3	2.078(4)	Zn2—N4	2.031(4)
Zn1—O2	1.994(4)	Zn2—O1W	2.209(4)

chemical bond	bond angle /($^\circ$)	chemical bond	bond angle /($^\circ$)
O2—Zn1—N3	91.55(16)	O1—Zn1—C7	28.67(16)
O1—Zn1—O2	58.11(15)	O6—Zn2—N4	143.51(15)
N3—Zn1—O1	149.53(14)	O6—Zn2—O1W	94.11(15)
O2—Zn1—C7	29.45(17)	N4—Zn2—O1W	90.31(15)
N3—Zn1—C7	120.97(17)		

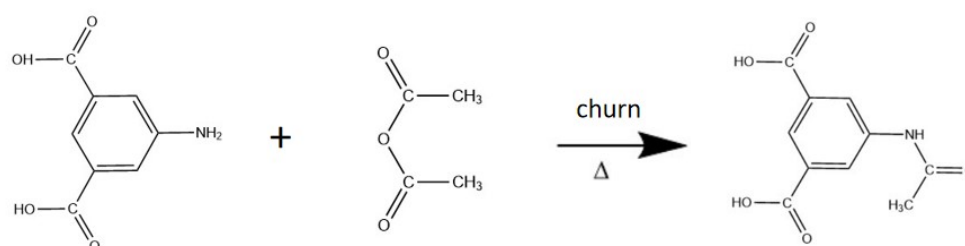


Fig. S1 Schematic diagram of the synthesis of H₂APA

In a 50 mL round bottom flask, 2.00 g of 5-amino-1,3-benzenedicarboxylic acid, 6 mL of acetic

anhydride and 6 drops of concentrated sulphuric acid were added respectively, and after initial mixing by shaking, a magnetic stirrer was added for stirring and the mixture was heated up to 90 °C in a water bath, and the reaction was carried out at 90 °C for 30 min, and then the reaction solution was quickly poured into 20 mL of cold distilled water and stirred to produce a precipitate, which was filtered and dried to give a white Solid (90% yield), that is, 5-acetamido-1,3-benzenedicarboxylic acid ligand (H₂APA).

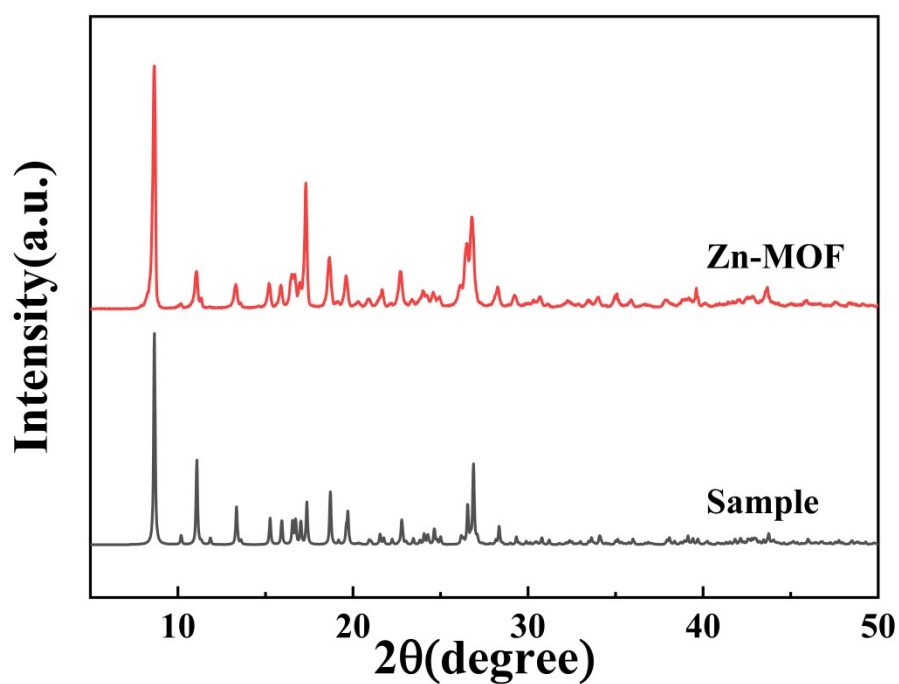


Fig. S2 XRD patterns of Zn-MOFs

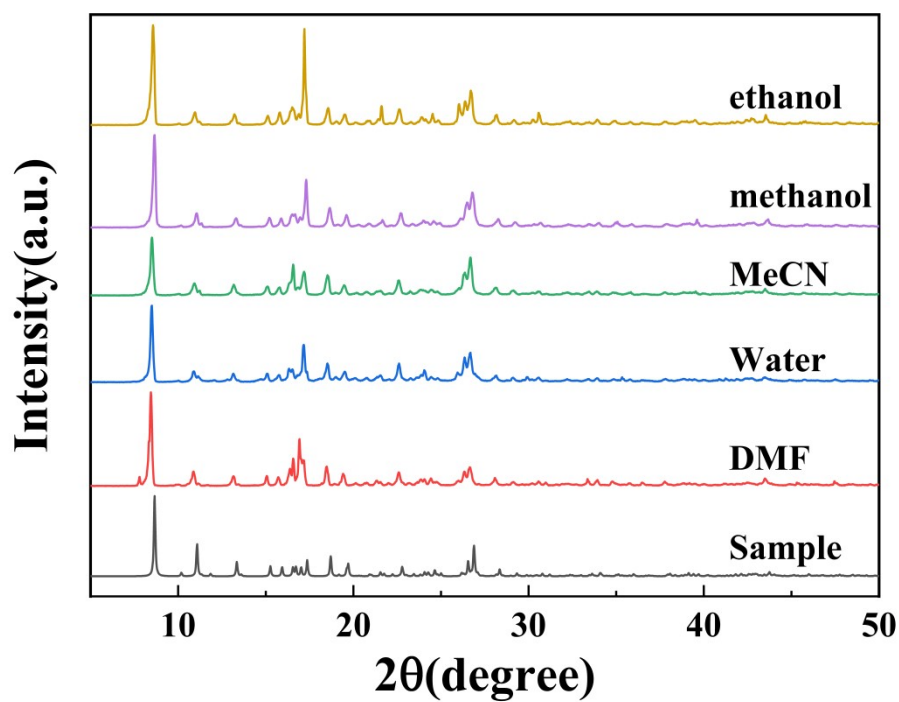


Fig. S3 XRD spectra of Zn-MOFs before and after immersion

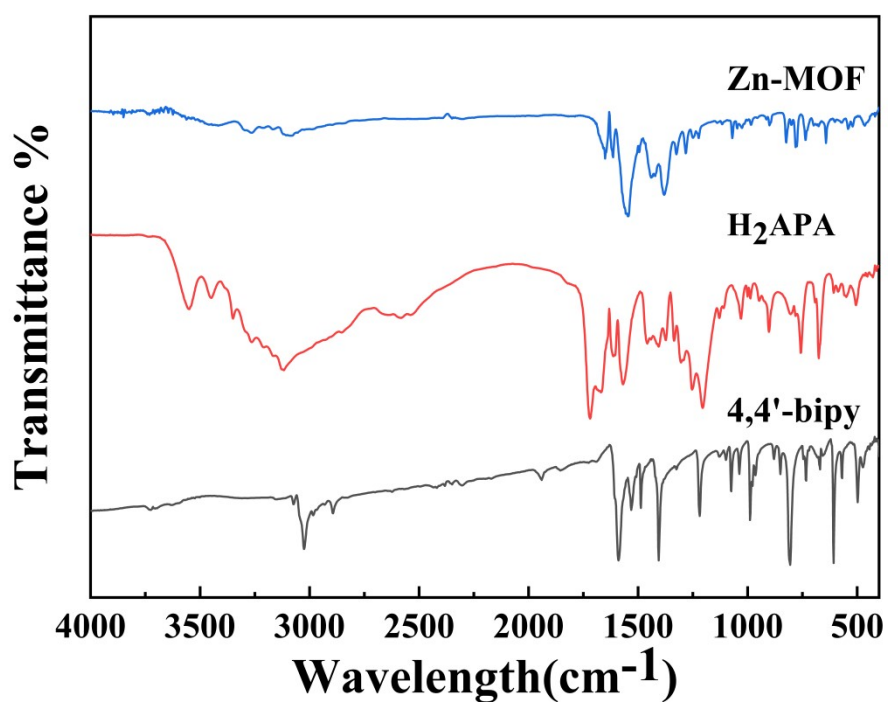


Fig. S4 Infrared spectra of ligands and complexes

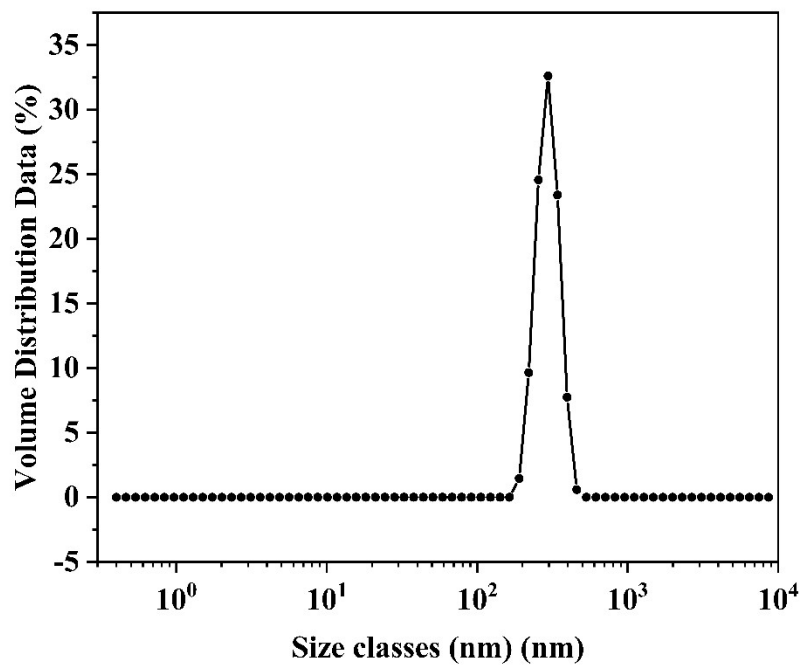


Fig. S5 The particle size distribution diagram in solution

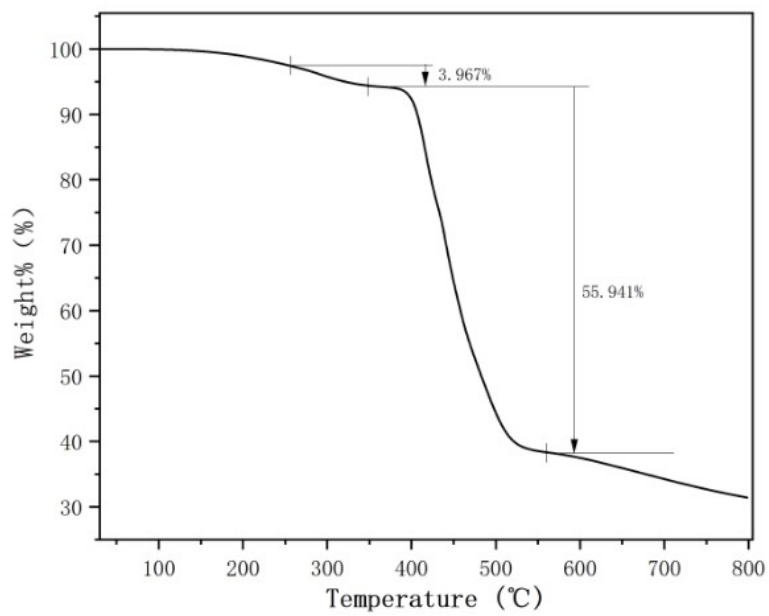


Fig. S6 Thermogravimetric curves of Zn-MOFs

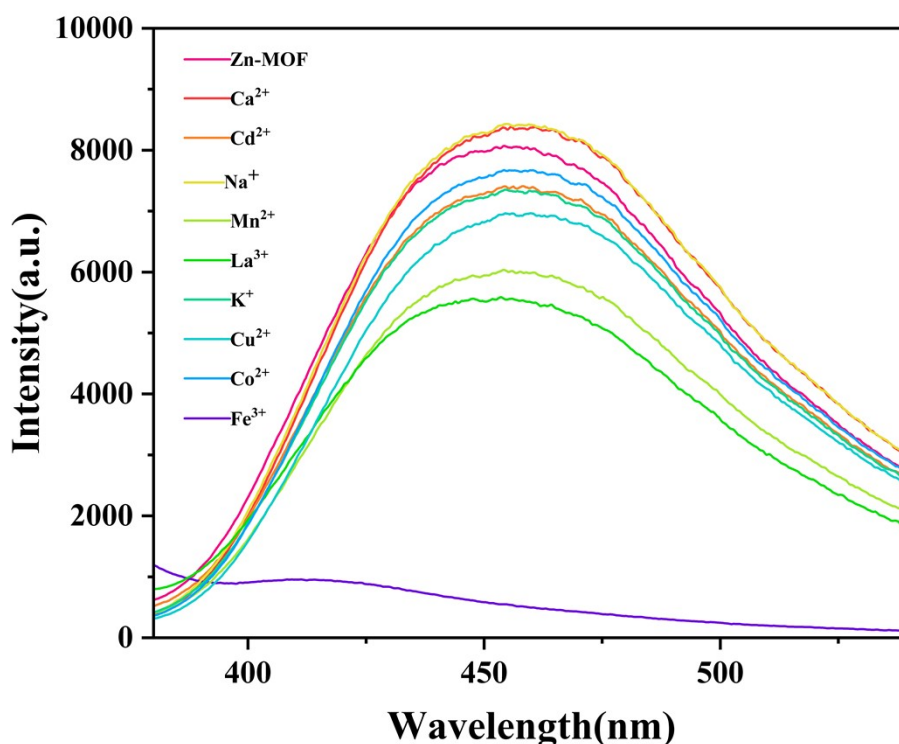


Fig. S7 Fluorescence Emission Spectrum Graph of Metal Ions

Table. S3 Price comparison of some MOFs that can quench Fe³⁺

CCDC number	sample name	total price of metal salts/ \$	total price of organicligands/ \$	price of organic solvents/ \$	cost of a 0.1 mmol sample/ \$
2396827	Zn-MOF	5.77×10^{-4}	0.022	7.73×10^{-3}	0.03
1573428	[Eu ₂ IJDMTDC) ₃ IJDEF) ₄]·DEF·6H ₂ O	0.085	7.00	0.6750	7.76
1573429	[Tb ₂ IJDMTDC) ₃ IJDEF) ₄]·DEF·6H ₂ O	0.208	7.00	0.6750	8.00
1521670	{(Me ₂ NH ₂)[Tb(OBA) ₂](Hatz)(H ₂ O) _{1.5}] _n }	0.220	0.016	0.0155	0.252
1565344	{[Eu ₂ (pdba) ₃ (H ₂ O) ₃]·2H ₂ O} _n }	0.0485	1.361	0.1156	1.525
1565345	{[Eu ₃ (pdba) ₄ (H ₂ O) ₄]·5H ₂ O} _n }	0.0485	1.362	0.1156	1.526
1509860	534-MOF-Tb	0.0988	5.968	0.8508	6.9176
1410772	[(CH ₃) ₂ NH ₂]·[Tb(bptc)]·x(solvents)	0.0274	0.551	0.3911	0.6175
1035886	Eu-BPDA	0.0436	0.0384	0.3265	0.4445
1965138	Eu-MOF	0.0582	0.0865	0	0.1447
1965139	Tb-MOF	0.2169	0.0865	0	0.3034
1056662	UiO-66-NH ₂	0.5437	0.4686	0.0231	1.035
2217760	{[Ag(L)]ClO ₄ ·H ₂ O} _n }	0.1842	6.0	0	6.1842

2217761	$\{\text{[Ag(L)]NO}_3 \cdot \text{H}_2\text{O}\}_n$	0.0617	6.0	0	6.0617
2217762	$\{\text{[Ag(L)]BF}_4 \cdot \text{H}_2\text{O}\}_n$	0.2202	6.0	0	6.2202
1916377	$\{\text{[Cd(5-Brp)(dpa)]} \cdot 0.5\text{DMF} \cdot \text{H}_2\text{O}\}_n$	0.0144	0.2282	2.884×10^{-4}	0.2429
1916379	$\text{[Cd(5-Brp)(bpp)(H}_2\text{O)]}_n$	0.0144	0.1818	5.047×10^{-4}	0.1967
2076041	Tb-MOF	0.1445	0.2971	0.0232	0.4648
1905642	$\text{[Cd}_{0.5}(\text{TBC})]_n$	0.1442	0.3954	0.2692	0.6790
1974695	Tb-MOF-A	0.2189	0.2173	0	0.4362
1846840	$\text{[Tb}_2(2,3'\text{-oba})_3(\text{phen})_2]_n$	0.2169	0.0882	0	0.3051

Solely the price parameters of chemical reagents are incorporated into consideration. The price details of all chemical reagents can be procured from Aladdin Reagents. In the realm of chemical synthesis, the computational process is predicated on the hypothesis of an ideal reaction, while the expenditure on electricity and water is omitted from the scope of consideration.

Table. S4 Comparison of LOD Values of Some MOFs that Can quench Fe^{3+}

CCDC number	sample name	LOD/mol·L ⁻¹
2396827	Zn-MOF	5.619×10^{-6}
2354330	CUST-761	2.98×10^{-4}
1509860	534-MOF-Tb	1.3×10^{-4}
1410772	$\text{[(CH}_3)_2\text{NH}_2] \cdot \text{[Tb(bptc)]} \cdot x(\text{solvents})$	1.8×10^{-4}
1974695	Tb-MOF-A	1.27×10^{-5}
1846840	$\text{[Tb}_2(2,3'\text{-oba})_3(\text{phen})_2]_n$	7.93×10^{-6}
2217760	$\{\text{[Ag(L)]ClO}_4 \cdot \text{H}_2\text{O}\}_n$	11.46×10^{-6}
2217761	$\{\text{[Ag(L)]NO}_3 \cdot \text{H}_2\text{O}\}_n$	15.83×10^{-6}
2217762	$\{\text{[Ag(L)]BF}_4 \cdot \text{H}_2\text{O}\}_n$	15.44×10^{-6}
1521670	$\{(\text{Me}_2\text{NH}_2)[\text{Tb}(\text{OBA})_2](\text{Hatz})(\text{H}_2\text{O})_{1.5}\}_n$	10^{-6}
2213445	$\{\text{[Cd(ttc)(H}_2\text{O)]} \cdot \text{H}_2\text{O}\}_n$	5.34×10^{-8}
1873450	$\text{[[Tb(Cmdcp)(H}_2\text{O})_3]_2(\text{NO}_3)_2 \cdot 5\text{H}_2\text{O}]_n$	4.0×10^{-6}
1899278	Eu-CP	5.0×10^{-7}
1818852	$\text{[Eu}_2\text{L(1,3-bdc)}_3] \cdot 5\text{H}_2\text{O}$	2.3×10^{-5}
1884067	$\text{[Eu}_2(\text{ppda})_2(\text{npdc})(\text{H}_2\text{O)]} \cdot \text{H}_2\text{O}$	1.66×10^{-5}
1821918	$\text{[Eu(IMS1)}_2]\text{Cl} \cdot 4\text{H}_2\text{O}$	2.3×10^{-5}
1035886	$\text{[[Eu(bpda)}_{1.5}] \cdot \text{H}_2\text{O}]_n$	0.9×10^{-6}
1538770	$\{\text{[Zn(ATA)(L)]}\}_n \cdot x\text{H}_2\text{O}$	3.76×10^{-6}
1538771	$\{\text{[Cd(ATA)(L)]}\}_n \cdot x\text{H}_2\text{O}$	1.77×10^{-6}
1542239	$\{\text{[Zn(DPTMIA)]} \cdot (\text{H}_2\text{O})_2(\text{DMF})_{0.5}\}_n$	1.09×10^{-3}
1840235	$\{\text{[Cd}_3(\text{HL})_2(\text{H}_2\text{O})_3] \cdot 3\text{H}_2\text{O} \cdot 2\text{CH}_3\text{CN}\}_n$	9.06×10^{-5}

Upon examination of the comparison table, it becomes manifestly evident that our Zn-MOF material exhibits a remarkably lower limit of detection (LOD) value with respect to Fe^{3+} . When juxtaposed

with the preponderant majority of MOFs, it conspicuously showcases a more preponderant advantage in the domain of LOD. This distinctive characteristic endows it with the capacity to effectuate a more exquisitely sensitive and highly accurate detection of Fe³⁺.

Notes and references

1. Huang, Y. Q.; Chen, H. Y.; Wang, Y.; Ren, Y. H.; Li, Z. G.; Li, L. C.; Wang, Y., *RSC Adv.*, **2018**, *8*, 21444–21450. DOI: 10.1039/c8ra02809e
2. Wang, J.; Wang, J. R.; Li, Y.; Jiang, M.; Zhang, L.; Wu, P., *New J. Chem.*, **2016**, *40*, 8600. DOI: 10.1039/c6nj02163h
3. Parmar, B.; Rachuri, Y.; Bisht, K. K.; Suresh, E., *Inorg. Chem.*, **2017**, *56*, 10939–10949. DOI: 10.1021/acs.inorgchem.7b01130
4. Li, H.; He, Y.; Li, Q.; Shao, S.; Yi, Z.; Xu, Z.; Wang, Y., *RSC Adv.*, **2017**, *7*, 50035. DOI: 10.1039/c7ra08427g
5. Yu, H. H.; Chi, J. Q.; Su, Z. M.; Li, X.; Sun, J.; Zhou, C.; Hu, X. L.; Li, Q., *CrystEngComm*, **2020**, *22*, 3638. DOI: 10.1039/d0ce00430h
6. Zhao, K. Y.; Zhai, X.; Shao, L.; Li, L.; Liu, Y. L.; Zhang, L. M.; Fu, Y., *J. Mater. Chem. C.*, **2021**, *9*, 15840. DOI: 10.1039/d1tc04311k
7. Wu, M. Z.; Shi, J. Y.; Chen, P. Y.; Tian, L., *New J. Chem.*, **2019**, *43*, 10575. DOI: 10.1039/c9nj02214g
8. Zhu, S. Y.; Yan, B., *Dalton Trans.*, **2018**, *47*, 11586. DOI: 10.1039/c8dt02051e
9. Jia, L.; Xue, Z.; Zhu, R. R.; Yan, T.; Wang, Y. N.; Zhang, S. S.; Du, L. X.; Zhao, Q. H., *RSC Adv.*, **2019**, *9*, 39854. DOI: 10.1039/c9ra07559c
10. Wu, J. M.; Ma, S. X.; Kumar, S.; Yang, Y.; Ren, P. T., *ACS Appl. Mater. Interfaces*, **2023**, *15*, 17317–17323. DOI: 10.1021/acsami.2c22871
11. Huang, Y. Q.; Chen, H. Y.; Wang, Y.; Ren, Y. H.; Li, Z. G.; Li, L. C.; Wang, Y., *RSC Adv.*, **2018**, *8*, 21444–21450. DOI: 10.1039/c8ra02809e

12. Wang, J.; Wang, J. R.; Li, Y.; Jiang, M.; Zhang, L.; Wu, P., *New J. Chem.*, **2016**, *40*, 8600. DOI: 10.1039/c6nj02163h
13. Parmar, B.; Rachuri, Y.; Bisht, K. K.; Suresh, E., *Inorg. Chem.*, **2017**, *56*, 10939–10949. DOI: 10.1021/acs.inorgchem.7b01130
14. Li, H.; He, Y.; Li, Q.; Shao, S.; Yi, Z.; Xu, Z.; Wang, Y., *RSC Adv.*, **2017**, *7*, 50035. DOI: 10.1039/c7ra08427g
15. Yu, H. H.; Chi, J. Q.; Su, Z. M.; Li, X.; Sun, J.; Zhou, C.; Hu, X. L.; Li, Q., *CrystEngComm*, **2020**, *22*, 3638. DOI: 10.1039/d0ce00430h
16. Zhao, Y. M.; Zhai, X.; Shao, L.; Li, L.; Liu, Y. L.; Zhang, X. M.; Fu, Y., *J. Mater. Chem. C.*, **2021**, *9*, 15840. DOI: 10.1039/d1tc04311k
17. Wu, M. Z.; Shi, J. Y.; Chen, P. Y.; Tian, L., *New J. Chem.*, **2019**, *43*, 10575. DOI: 10.1039/c9nj02214g
18. Zhu, S. Y.; Yan, B., *Dalton Trans.*, **2018**, *47*, 11586. DOI: 10.1039/c8dt02051e
19. Jia, L.; Xue, Z.; Zhu, R. R.; Yan, T.; Wang, Y. N.; Zhang, S. S.; Du, L. X.; Zhao, Q. H., *RSC Adv.*, **2019**, *9*, 39854. DOI: 10.1039/c9ra07559c
20. Mohan, B.; Ma, S. X.; Kumar, S.; Yang, Y.; Ren, P. T., *ACS Appl. Mater. Interfaces*, **2023**, *15*, 17317–17323. DOI: 10.1021/acsami.2c22871